Polish Society of Composite Materials
Polskie Towarzystwo Materiałów Kompozytowych

24: 1 (2024) 39-48

COMPOSITES THEORY AND PRACTICE

ISSN (online): 2299-128X

Ufuk Demircioğlu*, Mutlu Tarık Çakır

[1] *Sivas University of Science and Technology, Faculty of Engineering and Natural Sciences, Department of Mechanical Engineering, Sivas, Turkey*
**Corresponding author: E-mail: udemircioglu@sivas.edu.tr*

Received (Otrzymano) 8.11.2023

INVESTIGATION OF THE INFLUENCE OF DEBONDING SHAPES AND DEBONDING LOCATIONS ON VIBRATION BEHAVIOR OF SANDWICH STRUCTURE

https://doi.org/10.62753/ctp.2024.06.1.1

Sandwich structures are employed in many different fields including automobile, marine, and aircraft structures. However, debonding may take place at the core-face sheet interface, reducing the stiffness of the structure. Debonding may occur for a variety of reasons, including initial manufacturing faults, changes in service loads, tool drops, and foreign object impacts. It is critical to comprehend how debonding zones impact the vibration of sandwich structures because decreases in the natural frequencies (NF) could lead to a structure vibrating at resonance and lead to structural failure. This paper investigates the influence of debonding shapes and debonding locations on the free-vibration behavior of sandwich structures. Different sandwich structures that have varied debonding shapes at various locations are modeled using COMSOL MULTIPHYSICS. Debonding is modeled by using the CZM model. Validation studies were performed to validate the current study. After the validation study, free vibration analysis of all the sandwich structures was performed and the first six NF were obtained from the simulations. The results show the influence of the debonding shapes and debonding locations on the NF of the sandwich structures. From the results, it was observed that both the debonding shapes and debonding locations significantly change the NF of the sandwich structures. The debonding shapes cause a reduction and an increase depending on the debonding location. It was also revealed that both debonding shapes and debonding locations have a significant effect on the vibration behavior of sandwich structures. Using this method, the debonding shape and location, delamination shape, and location can be predicted using machine learning algorithms. This study includes free vibration analysis of sandwich structures with different debonding shapes and locations, and the results show that natural frequencies change depending on the debonding shapes and locations. This information can be implemented in machine learning for use in the field of damage detection and utilized to predict the shape and location of delamination in sandwich structures.

Keywords: delamination, delamination shapes, delamination locations, sandwich structures, vibration analysis

INTRODUCTION

Nowadays, development in industry is of utmost importance. Technology, which is always evolving, calls for sophisticated materials. As a result of this, researchers are looking for improved materials [1, 2]. When excellent damping qualities, manufacturing diversity, fatigue resistance, high stiffness-to-weight, and strength-to-weight ratios are sought, sandwich structures are one of the top candidates to replace conventional materials [3, 4]. Sandwich structures are heterogeneous composite structures comprised of two or more different types of materials. When the qualities of many materials are combined, they provide qualities that are superior to those of each material alone [5]. Since sandwich structures provide better mechanical properties than their monolithic components and conventional materials, they are used especially in aviation, and marine applications. However, due to the chosen manufacturing method of the sandwich structure, some problems like unbonded regions occur. Because of environmental effects, a part of the sandwich structure could be damaged. Also, as a consequence of the application field where sandwich structures are used, they are mostly under dynamic loadings [6]. Therefore, it is important to study and evaluate the dynamic characteristics of sandwich structures under the assumption that the sandwich structure has undergone debonding. Debonding is one of the most serious flaws in sandwich structure materials [7]. Debonding, which occurs between the face and the core, might be a major challenge for designers. Debonding causes could be related to problems with the initial production or with service loads. Debonding may significantly reduce the load-bearing capacity of sandwich structures and have an impact on their mechanical behaviors. It is therefore important to investigate the influence of debonding on the dynamic performance of sandwich structures.

There are many accounts of investigations on the free vibration of sandwich structures with debonding in the literature. For example, Mohanan et al. studied the effectiveness of sandwich structures in the presence of

debonding and dents. ANSYS 13.0. was used to evaluate the buckling load factor, NF, mode shape, and modal strain energy. From the study, it was observed that debonding affects the performance of a sandwich structure more adversely than dents. It was also found that the presence of debonding and dents do not significantly affect the NF; nevertheless, debonding causes a significant reduction in the buckling load factor [8]. Moustapha et al. evaluated the damping of sandwich structures in the presence of debonding. The influence of debonding with different lengths on the NF and damping was evaluated experimentally and numerically. From the results, it was found that debonding significantly affects the NF and damping of sandwich structures [9]. Baba investigated the influence of debonding on the free vibration of flat and curved sandwich structures by experimental and numerical methods. From the results, it was concluded that debonding and curvature angles have a significant effect on NF. Also, it was observed that debonding causes a reduction in the NF of sandwich structures [10]. Burlayenko and Sadowski investigated the vibration behavior of sandwich structures with debonding at the core-face sheet interface. The study was conducted using the finite element method in ABAQUS software. Under different boundary conditions, the effects of debonding, size, and location on the free vibration behavior of sandwich structures were evaluated [11]. Kim and Hwang investigated the influence of debonding on the NF and on the flexural bending stiffness of the sandwich structure. A split sandwich beam model was employed in the study. Flexural stiffness and NF were studied in relation to the level of debonding. From the results, it was concluded that increasing face sheet layer debonding reduces the flexural stiffness of sandwich structures. Moreover, it was found that increasing the extent of debonding reduces the NF of sandwich structures [12]. Baba and Thoppul examined how curvatures and debonding affected the stiffness and strength of composite sandwich beam constructions. Four-point bending and the impulse frequency response approach were employed to evaluate the flexural stiffness and strength. According to the results of vibration tests, curvature, and debonding have a minimal impact on NF and the apparent stiffness but have a considerable impact on loss factors [13]. Tsai and Taylor investigated the effect of debonding on the NF of flat and curved sandwich structures. Flat and curved sandwich structures were subjected to hammer impact tests and finite element simulations. From the results, it was observed that both curvature and debonding have an effect on the NF of sandwich structures [14]. Burlayenko and Sadowski studied the free vibration of a sandwich plate having single/multiple debonding. ABAQUS software was used to calculate the dynamic properties of sandwich plates with and without debonding, including the NF and corresponding mode shapes. The influence of the size, location, and number of sites with debonding on the dynamic behavior of sandwich structures was ascertained [15]. Sadeghpour et al. investigated the vibration behavior of a debonded curved sandwich structure. The governing equations were derived and solved by means of the Rayleigh-Ritz method and the Lagrange principle. Finite element software ANSYS Workbench was utilized to verify the results. The analyses show that the curvature angle and boundary conditions have a significant impact on how a curved beam responds to vibration. The findings also demonstrate that the debonding effect on the NF is about the same for both flat and curved beams [16]. Tsai and Taylor researched the vibration behavior of sandwich structures that have single and double debonding. To analyze the vibration characteristics of sandwich structures, impact tests, and finite element methods were carried out. From the results, it was found that the debonded parts reduced the fundamental frequencies of the sandwich structures [17]. Idriss et al. studied the vibration behavior of sandwich structures with debonding regions. Linear and nonlinear vibration methods were employed in the study. The findings demonstrated that compared to the linear parameters, the nonlinear parameters were substantially more sensitive to damage [18]. Tsai researched the effect of different face sheet-core interface delamination configurations and face sheet arrangement orientations on the vibration behavior of composite sandwich beams. The findings revealed that maintaining distance between delaminations affected the vibration node position, an effect that resulted in larger reductions in the natural frequencies [19]. Kalgutkar and Banerjee investigated the free vibration of stiffened composite plates under hygrothermal conditions, emphasizing interfacial debonding at the plate-stiffener interface. Utilizing a simplified finite element model, the research considered three laminate schemes and revealed that extreme environmental conditions notably affect the natural frequency of the panel. The developed model proved to be computationally efficient, offering insights into the free vibration behavior of the debonded stiffened panel in hygrothermal environments [20].

When the literature is taken into consideration, the effects of debonding have been investigated by the researchers as previously mentioned. The shape, length, and location of debonding are important parameters. Even though the length of debonding has been investigated, there is no study that investigated the influence of the shape and location of debonding on the NF of sandwich structures. Therefore, this study aims to numerically evaluate the effects of the location and shape of debonding on the NF of sandwich structures.

Motivation

The motivation behind the study is driven by the importance of sandwich structures in various industries, including automobile, marine, and aircraft applications. Sandwich structures are valued for their excellent damping qualities, manufacturing diversity, and fatigue resistance, in addition to high stiffness-to-weight and strength-to-weight ratios. Nonetheless, debonding,

which can occur at the core-face sheet interface, poses a significant challenge, potentially reducing the stiffness of the structures. The study aims to understand how different debonding shapes and locations impact the free-vibration behavior of sandwich structures.

Novelty

The novelty of the study lies in its investigation of the combined effects of debonding shapes and locations on the natural frequencies of sandwich structures. While previous research has explored the impact of debonding on these structures, the specific focus on the shape and location of debonding as key parameters makes this study unique. The authors utilize numerical simulations and finite element analysis, implemented by means of COMSOL Multiphysics, to model and analyze sandwich structures with various debonding shapes and locations.

The subsequent sections are as follows: in the Material and Methods section of the study, the parameters, modeling process, and debonding scenarios of the simulations performed with COMSOL MULTIPHYSICS software are explained in detail. Additionally, the physical properties and material components of the sandwich structure samples are specified. In the Results section, the findings obtained by means of these methods and the effects of different debonding methods are briefly summarized.

MATERIALS AND METHODS

In this study, the finite element method was used. Different sandwich structures were modeled using COMSOL MULTIPHYSICS as shown in Figure 1 to evaluate the effects of the debonding shape and its location on the vibration behavior of sandwich structures. The configuration of sandwich structures was 90°/0°/*Foam*/ 0°/90°. Glass fiber and polyvinyl chloride (PVC) foam were used for the face sheet and core materials, respectively. The thickness of the glass fiber and PVC foam were 0.2 mm and 10 mm, respectively. The length of the sandwich structures was 300 mm, while the width was 30 mm. The properties of the materials used in the study are given in Table 1. Free vibration analysis was carried out in COMSOL MULTIPHYSICS to obtain the NF. The analysis was performed under cantilever boundary conditions. Debonding in sandwich structures can be modeled by using a cohesive zone model (CZM). Hence, in this study, CZM was implemented by means of COMSOL MULTIPHYSICS and using the parameters in [21]. CZM is a widely used modeling approach for the analysis of damage and separation processes at material interfaces. This model helps us understand and simulate the behavior of debonding formed at the material interface. Debonding was assigned at 20 mm intervals along its length from the fixed end (20 mm from the fixed end) to the free end (280 mm from the fixed end) of the sandwich structure through its center using a parameter sweep tool (Fig. 1). Different-shaped delamination was introduced to the sandwich structures as shown in Figure 1. All the delamination shapes have the same area (314 mm^2).

TABLE 1. **Properties of materials considered for analysis [22]**

Property	Glass fiber	PVC foam
Density [kg/m^3]	2000	60
Young's modulus E_x [Pa]	4.5e+10	7e+07
Young's modulus E_y [Pa]	1e+10	-
Young's modulus E_z [Pa]	1e+10	-
Poisson's ratio v_{xy}	0.3	0.3
Poisson's ratio v_{yz}	0.4	0.3
Poisson's ratio v_{zx}	0.3	0.3
Modulus of rigidity G_{xy} [Pa]	5e+09	2.6923e+07
Modulus of rigidity G_{xz} [Pa]	3.8462e+09	2.6923e+07
Modulus of rigidity G_{yz} [Pa]	5e+09	2.6923e+07

The data obtained from the simulation is too big to present in this paper, therefore the statistical properties: the mean, standard deviation (SD), and minimum and maximum values of each sandwich sample are presented in Table 2.

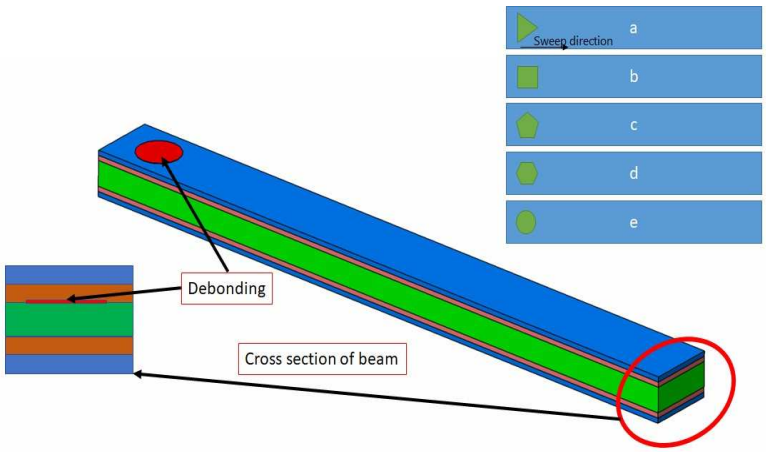

Fig. 1. Debonding: a) triangular debonding, b) rectangular debonding, c) pentagonal debonding, d) hexagonal debonding, and e) circular debonding

TABLE 2. **Statistical properties of sandwich samples**

Delamination shape	Statistical properties	Mode 1 [Hz]	Mode 2 [Hz]	Mode 3 [Hz]	Mode 4 [Hz]	Mode 5 [Hz]	Mode 6 [Hz]
Circular	Mean	97.04	171.71	487.29	504.26	999.20	1103.82
	std	0.1034	0.1417	2.9292	3.1036	1.6149	8.210
	Max	97.147	171.840	489.700	507.440	1001.500	1111.400
	Min	96.814	171.400	480.460	498.150	996.630	1081.900
Triangular	Mean	97.0047	171.64	486.862	502.616	999.428	1102.992
	std	0.0536	0.0611	1.8926	1.2461	0.9202	5.7442
	Max	97.056	171.800	488.200	505.400	1001.400	1107.200
	Min	96.860	171.57	481.920	500.920	998.179	1086.300
Rectangular	Mean	96.996	171.632	486.702	502.485	999.501	1102.414
	std	0.0493	0.0536	1.8059	1.2157	1.9603	5.1953
	Max	97.059	171.790	488.030	506.320	1005.200	1106.800
	Min	96.895	171.540	482.460	500.690	997.820	1088.300
Pentagonal	Mean	97.015	171.662	486.846	503.282	998.979	1102.328
	std	0.1031	0.1461	3.0397	2.8423	1.8301	8.6238
	Max	97.124	171.870	489.760	508.320	1002	1110.400
	Min	96.780	171.340	479.710	497.600	995.970	1079.300
Hexagonal	Mean	97.021	171.692	487.167	503.459	999.612	1103.878
	std	0.0637	0.0712	2.0786	1.3462	0.8044	6.0990
	Max	97.101	171.850	489.040	506.470	1001.300	1110.200
	Min	96.867	171.550	481.880	501.010	998.100	1086.700

Governing equation

In this section, the equation of motion for a sandwich structure is explained. The mathematical model was adopted from [23]. Sandwich beam cross sections have two symmetry axes, y, and z. Sandwich construction with two symmetrical cross sectional planes may experience flexural vibration in one plane and torsional vibration in the other. There are 3 sets of vibrations, namely, $w_1 = w_y$, $w_2 = w_z$ and $w_3 = w_\psi$. Where w_1 and w_2 represent the vibration in the $x - z$ and $x - y$ planes, respectively, and w_3 is torsional vibration. In this paper, just the vibration in the $x - z$ plane is given. The following are the equilibrium equations:

$$\begin{aligned} \frac{\partial w^o}{\partial x} &= x_{xz} + \gamma_{xz} \\ \frac{dV_x}{dx} + \rho\left(2\pi f\right)^2 w^o &= 0 \\ \frac{dM_x}{dx} - V_x &= 0 \end{aligned} \tag{1}$$

where x_{xz} and γ_{xz} are the rotation of the normal in the $x - z$ plane and transverse shear strain, respectively. w^o is the deflection and ρ is the mass per unit, M_x represents the bending moment of the beam, and V_x represents the shear force.

The bending moment of the sandwich beam and the transverse shear force for a symmetrical plate are as follows:

$$M_x = -D_{11}\frac{\partial_{x_{xz}}}{\partial_x},\ V_x = \overline{S}_{11}\gamma_{xz} \tag{2}$$

Equations (2), (3) along with Eq. (1) give the following equation along with compliance matrix S_{11} and stiffness matrix D_{11}

$$\begin{aligned} -D_{11}\frac{d^3x_{xz}}{dx^3} + \rho\left(2\pi f\right)^2 w^o &= 0 \\ D_{11}\frac{d^2x_{xz}}{dx^2} + \overline{S}_{11}\left(\frac{dw^0}{dx} x_{xz}\right) &= 0 \end{aligned} \tag{3}$$

The related equations for a sandwich beam in vibration are as follows:

$$\begin{aligned} -EI\frac{d^3x}{dx^3} + \rho'\left(2\pi f\right)^2 w &= 0 \\ EI\frac{d^2x}{dx^2} + S\left(\frac{dw}{dx} - x\right) &= 0 \end{aligned} \tag{4}$$

where EI and S are the bending and shear stiffness of the sandwich structure and ρ' is mass per unit length.

When D_{11}, S_{11}, and ρ are substituted with EI, S, and ρ', the equations describing the vibration of a sandwich structure (symmetrical layup) and an isotropic sandwich beam are identical.

Rearranging Eq. (5) by considering $p = \rho(2\pi f)^2 w^o$ Eq. (6) is obtained

$$\begin{aligned} -EI\frac{d^3x}{dx^3} + p &= 0 \\ EI\frac{d^2x}{dx^2} + S\left(\frac{dw}{dx} - x\right) &= 0 \end{aligned} \tag{5}$$

Equation (6) can be rearranged as follows:

$$\frac{1}{\rho w^2}\frac{d^4x}{dx^4}+\frac{1}{S}\frac{d^2x}{dx^2}-\frac{1}{EI}x=0 \tag{6}$$

$$w=\frac{EI}{\rho w^2}\frac{d^3x}{dx^3} \tag{7}$$

The solution of Eq. (7) is:

$$\begin{aligned}x=&C_1\cos h\frac{v}{L}x+C_2\sin h\frac{v}{L}x\\&+C_3\cos\frac{\mu}{L}x+C_4\sin\frac{\mu}{L}x\end{aligned} \tag{8}$$

When this equation is substituted in Eq. (8), the following expression is obtained:

$$\begin{aligned}w=\frac{EI_{yy}}{\rho w^2}\Bigg(&C_1\frac{v^3}{L^3}\sinh\frac{v}{L}x+C_2\frac{v^3}{L^3}\cosh\frac{v}{L}x\\&+C_3\frac{\mu^3}{L^3}\sin\frac{\mu}{L}x-C_4\frac{\mu^3}{L^3}\cos\frac{\mu}{L}x\Bigg)\end{aligned} \tag{9}$$

where L is the overall length of the sandwich structure and C_1-C_4 are constants that are ascertained from the boundary conditions; μ and v are determined as follows:

$$\mu=L\sqrt{\left(\frac{\rho w^2}{2S}\right)+\sqrt{\left(\frac{\rho w^2}{2S}\right)^2+\left(\frac{\rho w^2}{EI}\right)}} \tag{10}$$

$$v=L\sqrt{-\left(\frac{\rho w^2}{2S}\right)+\sqrt{\left(\frac{\rho w^2}{2S}\right)^2+\left(\frac{\rho w^2}{EI}\right)}} \tag{11}$$

From Eq. (11) the following is obtained:

$$\frac{1}{w^2}=\rho\left[\left(\frac{L}{\mu}\right)^2\frac{1}{EI}+\left(\frac{L}{\mu}\right)^2\frac{1}{S}\right] \tag{12}$$

When Eqs. (11) and (12) are combined, the following equation is obtained:

$$\mu^2-\frac{EI}{SL^2}\mu^2v^2-v^2=0 \tag{13}$$

Equations (9), (10), (13), and (14), along with the boundary conditions, give the frequencies of the sandwich structure.

RESULTS AND DISCUSSION

The numerical method is time and money-consuming compared to experimental study. However, one cannot rely on it. The accuracy of the finite element approach should be verified by experiment or by contrasting the findings with those found in the literature. Validation is done in this study by comparing the findings with those provided in [24]. Furthermore, the COMSOL MULTIPHYSICS results are compared with ANSYS ADPL results to ensure the accuracy of the finite element method. Table 3 presents the findings.

TABLE 3. **Comparison of results**

Natural frequencies [Hz]	Reference [24]	ANSYS ADPL	COMSOL
Mode 1	35.055	35.054	35.078
Mode 2	126.4	126.39	126.65
Mode 3	218.46	218.45	218.66
Mode 4	420.57	420.54	421.58
Mode 5	606.05	606.00	606.88

After the validation studies, a series of parametric studies was performed. The first six NF of each previously mentioned sandwich structure were obtained. Figures 2-7 show the results. The results are plotted with the x-axis showing the distance from the fixed end and the y-axis showing the NF. Figures 2 to 7 present the variation of Modes 1-6 depending on the distance from the fixed end, respectively. Generally speaking, NF increases as the distance from the fixed end goes from 0.020 m to 0.280 m in the sandwich structures with debonding. In general, it is seen that the debonding shapes have a major effect on the NF of the sandwich structure as seen in Figures 2-7.

When the debonding shape is considered, it is seen from Figures 2 through 7 that the influence of the debonding shape differs depending on the vibration mode of the sandwich structures. When Mode 1 of all the sandwich structures is considered, nearly all the debonding shapes cause a reduction in NF in all the locations when compared to the sandwich structure without debonding. Only the circular debonding at 0.260 m gives higher frequencies than the sandwich structure without debonding. In Modes 2-4 still the sandwich without debonding has a higher NF than the debonded sandwich structures other than a few points shown in Figures 3-5. The influence of the debonding shapes greatly fluctuates in Mode 5. The NF are higher or lower than the sandwich structure without debonding, depending on the debonding locations and debonding shapes. As shown in Figure 6, the effect of debonding causes an increase or decrease in the NF of the sandwich structures based on the location with respect to the sandwich structure without debonding. In Mode 6, the shapes of debonding as shown in Figure 7 reduce the NF in all the modes at all the locations other than the circular debonding at 0.22 m. Overall, the NF of the sandwich structures are sensitive to the debonding shapes.

When the debonding locations are taken into consideration, it is clearly seen from Figures 2-7 that the locations of debonding exhibit a significant effect on the vibration characteristics of the sandwich beam. In general, as the debonding goes from the fixed to the free end, the NF fluctuate depending on the mode numbers of the sandwich structures. It is clearly seen in Figure 2 that in Mode 1 the

NF tend to increase as the debonding goes from 0.020 mm to 0.280 mm. Nevertheless, the NF are still less than the sandwich structure without debonding at all the locations other than the circular debonding at location 0.260 m. In Mode 2 as shown in Figure 3, the NF of the sandwich structures with debonding fluctuates along the sweep distance with respect to the sandwich structure without debonding. Modes 3 and 6 of the sandwich structures have a similar trend as shown in Figures 4 and 7.

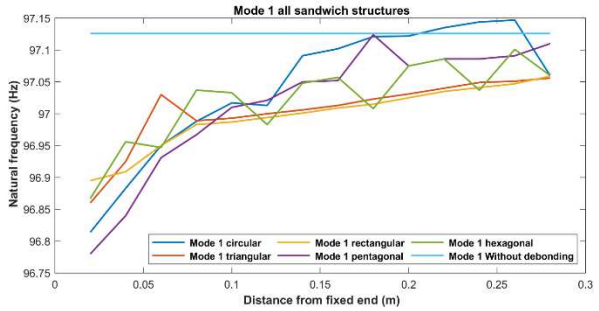

Fig. 2. Comparison of Mode 1 of sandwich structures along sweep distance

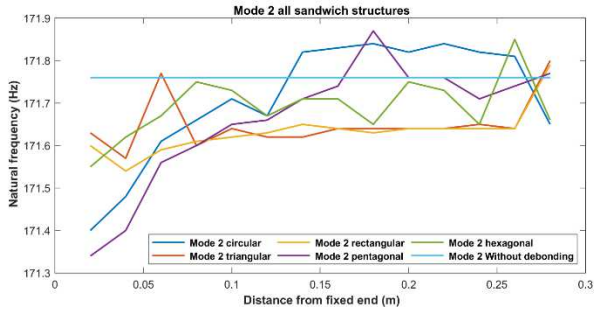

Fig. 3. Comparison of Mode 2 of sandwich structures along sweep distance

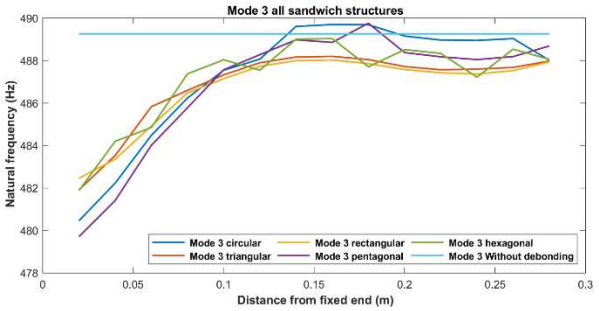

Fig. 4. Comparison of Mode 3 of sandwich structures along sweep distance

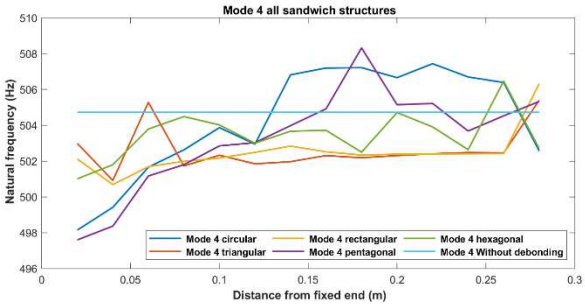

Fig. 5. Comparison of Mode 4 of sandwich structures along sweep distance

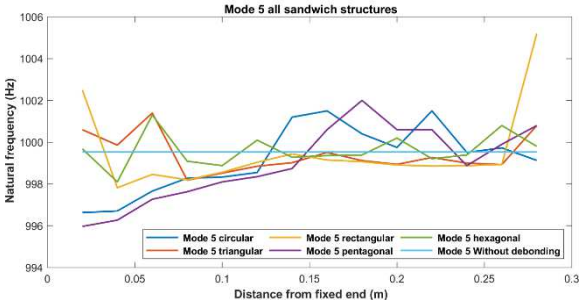

Fig. 6. Comparison of Mode 5 of sandwich structures along sweep distance

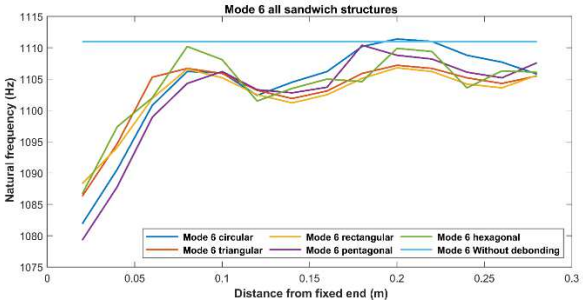

Fig. 7. Comparison of Mode 6 of sandwich structures along sweep distance

In these modes, the NF increase when the debonding location shifts from the fixed end to the free end. Modes 4 and 5 of the sandwich structures fluctuate randomly as shown in Figures 5 and 6 depending on the shape and location of debonding. On the whole, one can say that depending on the debonding location, the NF of the sandwich structures significantly vary.

Furthermore, each mode of sandwich structure is plotted at all the locations to the see variations in the NF depending on the debonding shapes. Figures 8 to 13 display the sandwich structures from Mode 1 to 6, respectively. When Mode 1 of all the sandwich structures with different debonding shapes and different locations is considered, one can see from Figure 8 that the NF are affected by both the debonding shapes and debonding locations. Even though the NF fluctuate slightly around 97 Hz, there seems to be a measurable difference. When Mode 2 is examined using Figure 9, the NF still fluctuate. Nonetheless, in Mode 2 the fluctuation is rather apparent. The effects of the debonding locations and debonding shapes are separated individually. In Mode 3, as the delamination locations change the NF significantly change depending on the delamination shape as shown in Figure 10. In this mode, the debonding shapes and debonding locations give unique natural frequencies.

Similar to Mode 3, in Mode 4 the NF of all the sandwich structures vary significantly as the debonding shape and debonding locations change as shown in Figure 11. One can see from Figure 12 that in Mode 5 the debonding location and debonding shapes exhibit a significant effect on the NF of the sandwich structures. The effects of the debonding locations and debonding shapes change uniquely. In Mode 6, as shown in Figure 13, the effect of the debonding shapes and debonding location is clearly seen. Furthermore, in this mode the effect of the parameters is rather apparent close to the fixed end.

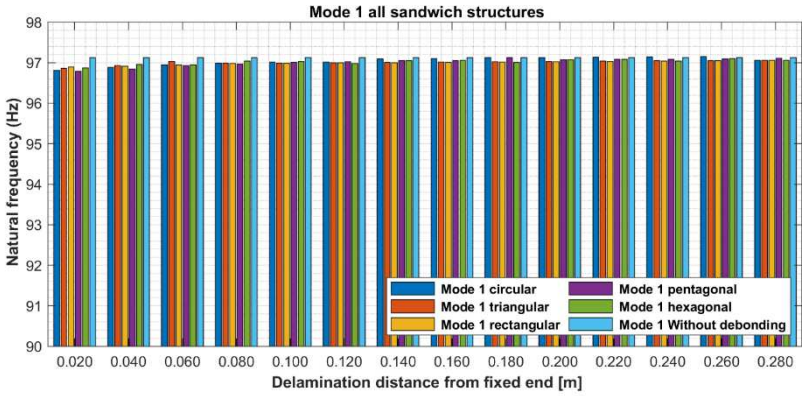

Fig. 8. Change in Mode 1 for various debonding shapes and debonding locations

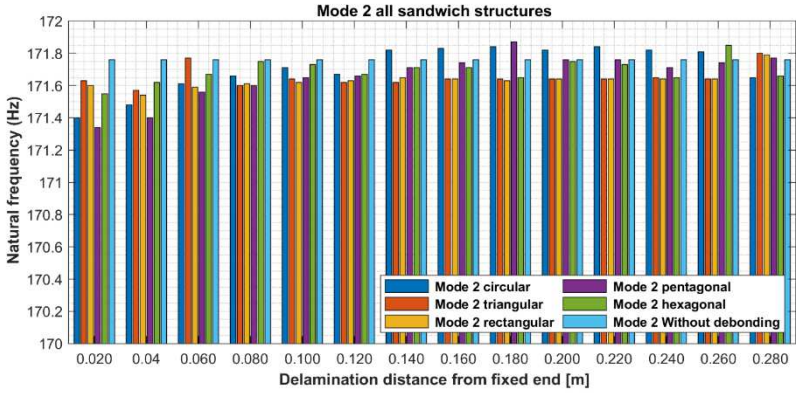

Fig. 9. Change in Mode 2 for various debonding shapes and debonding locations

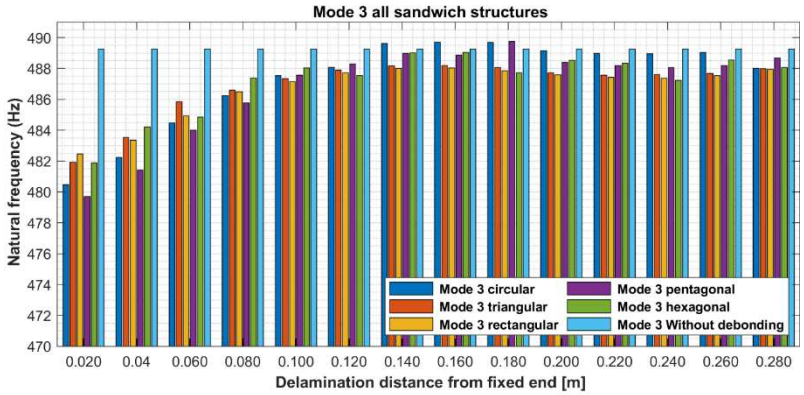

Fig. 10. Change in Mode 3 for various debonding shapes and debonding locations

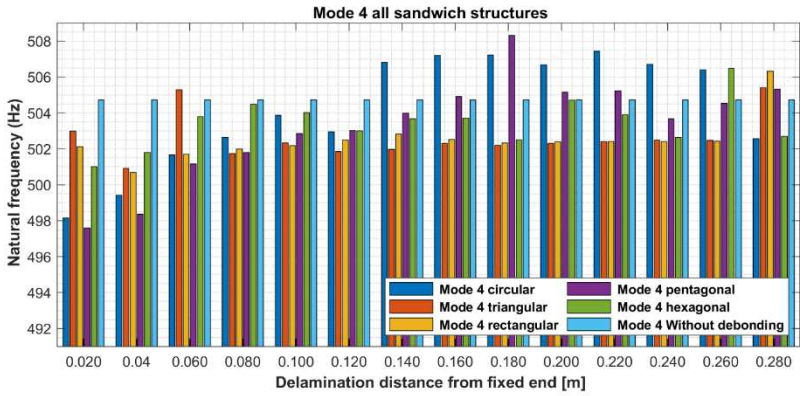

Fig. 11. Change in Mode 4 for various debonding shapes and debonding locations

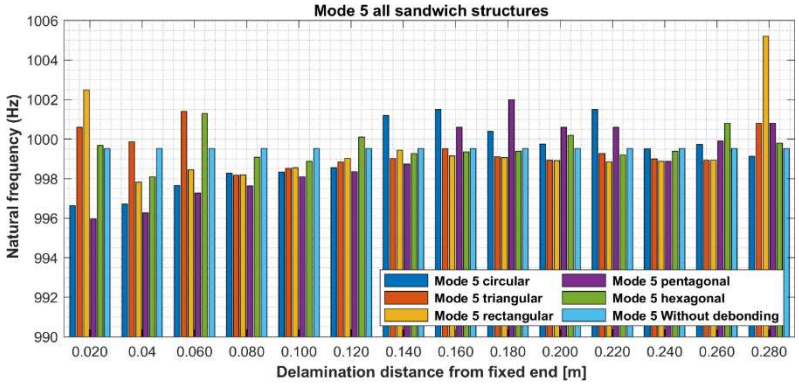

Fig. 12. Change in Mode 5 for various debonding shapes and debonding location

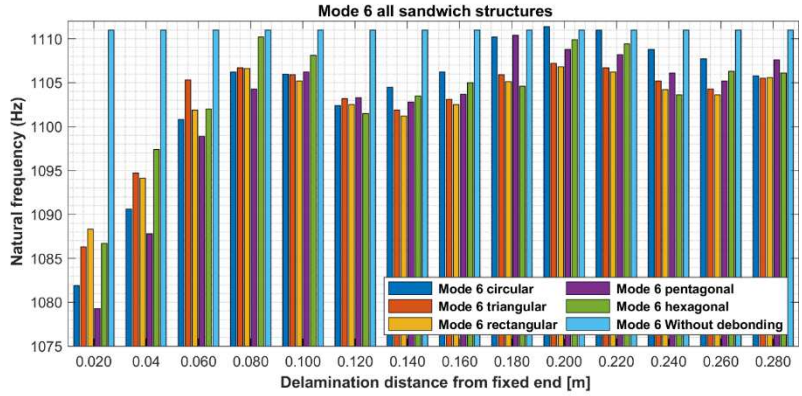

Fig. 13. Change in Mode 6 for various debonding shapes and debonding locations

Table 4 presents the maximum and minimum values of the NF of all the sandwich structures over the entire sweep. Using the values in Table 4, the percentage differences of each mode for each debonding shape are obtained and given in Table 5. Table 5 clearly shows the effect of the debonding shapes on the NF of the sandwich structures. This information can be very useful to determine the debonding shape. Also, as previously mentioned, the locations of debonding cause a change in the NF of the sandwich structure. On the whole, by using this method along with machine learning algorithms, one can easily detect the location and shape of debonding. In conclusion, the study systematically explored the effects of the debonding shapes and locations on the natural frequencies of the sandwich structures. The detailed analysis, complemented by comprehensive figures and tables, provides valuable insights for researchers and practitioners in the field.

TABLE 4. **Maximum and minimum values of each mode**

Delamination shape	Statistical properties	Mode 1 [Hz]	Mode 2 [Hz]	Mode 3 [Hz]	Mode 4 [Hz]	Mode 5 [Hz]	Mode 6 [Hz]
Circular	Max	97.14	171.84	489.70	507.44	1001.50	1111.40
	Min	96.81	171.40	480.46	498.15	996.63	1081.90
Triangular	Max	97.05	171.80	488.20	505.40	1001.40	1107.20
	Min	96.86	171.57	481.92	500.92	998.17	1086.30
Rectangular	Max	97.05	171.79	488.03	506.32	1005.20	1106.80
	Min	96.89	171.54	482.46	500.69	997.82	1088.300
Pentagonal	Max	97.12	171.87	489.76	508.32	1002	1110.400
	Min	96.78	171.34	479.71	497.60	995.970	1079.300
Hexagonal	Max	97.10	171.85	489.04	506.47	1001.300	1110.200
	Min	96.86	171.55	481.88	501.01	998.100	1086.700
Without debonding	--	97.12	171.76	489.26	504.73	999.53	1111.0

TABLE 5. **Percentage differences between maximum and minimum values of each mode**

Delamination shape	Mode 1	Mode 2	Mode 3	Mode 4	Mode 5	Mode 6
Circular delamination	0.34	0.25	1.92	1.86	0.48	2.72
Triangular delamination	0.20	0.13	1.30	0.89	0.32	1.92
Rectangular delamination	0.16	0.14	1.15	1.12	0.73	1.69
Pentagonal delamination	0.35	0.30	2.09	2.15	0.60	2.88
Hexagonal delamination	0.2	0.17	1.48	1.08	0.32	2.16

CONCLUSIONS

In this study, the free vibration analysis of sandwich structure with debonding was performed using numerical simulation. The finite element method was utilized to examine the free vibration properties of a sandwich beam with different debonding shapes and different debonding locations. The study focused on revealing the influence of various debonding shapes and debonding locations on the NF of the sandwich structure. COMSOL MULTIPHYSICS software was used to obtain the first six NF of the sandwich structures. Sandwich structures both without debonding and with debonding having different debonding shapes were modeled and solved using COMSOL MULTIPHYSICS. From the results, it was observed that the NF of the sandwich structures change as the debonding shape and debonding location change. The natural frequencies decrease or increase depending on the debonding shapes and debonding locations. This information is useful in damage detection. For example, one can employ this data in machine learning and use it in delamination shape and location prediction. To further confirm the accuracy of the dynamic response to identify the debonding issue in the sandwich construction, future research will integrate debonding modeling with experimental examination. Furthermore, machine learning algorithms will be used to detect the location and shapes of debonding in sandwich structures. While this study provides valuable insights into the free vibration analysis of sandwich structures with debonding, it is crucial to acknowledge certain limitations. The finite element method and specific debonding scenarios employed in numerical simulations may not fully represent real-world complexities. Generalizing the findings beyond the studied cases should be approached cautiously. The use of COMSOL MULTIPHYSICS, while effective, introduces computational limitations. Additionally, the application of machine learning for damage detection relies on robust datasets and faces challenges related to real-world variability and model complexity. Future research should focus on experimental validation and address practical issues to enhance the applicability of the proposed methods.

REFERENCES

[1] Hadji L., Avcar M., Zouatnia N., Natural frequency analysis of imperfect FG sandwich plates resting on Winkler-Pasternak foundation, Materials Today: Proceedings 2022, 53, 153-160.

[2] Hadji L., Avcar M., Free vibration analysis of fg porous sandwich plates under various boundary conditions, Journal of Applied and Computational Mechanics 2021, 7, 2, 505--519, DOI: 10.22055/jacm.2020.35328.2628.

[3] Kumar A., Angra S., Chanda A.K., Stress properties optimization of a composite sandwich structure by application of hybrid Taguchi-GRA-PCA, Journal of Engineering Research 2021, 9, 203-216, DOI: 10.36909/jer.EMSME.13875.

[4] Vaisali M.S., Nisha A.S., Damage detection using modal strain energy method in honeycomb sandwich beams with multiple delaminations, IJISET-International Journal of Innovative Science, Engineering & Technology 2015, 2, 7, 533-554.

[5] Avcar M., Hadji L., Civalek Ö., Natural frequency analysis of sigmoid functionally graded sandwich beams in the framework of high order shear deformation theory, Composite Structures 2021, 276, June, DOI: 10.1016/j.compstruct.2021.114564.

[6] Thomas T., Tiwari G., Performance evaluation of reinforced honeycomb structure under blast load, Journal of Engineering Research 2021, 1-26, DOI: 10.36909/jer.11929.

[7] Burlayenko V.N., Sadowski T., Numerical modeling of dynamics of sandwich plates with partially debonded skin-to-core interface for damage detection, Proceedings of the 8th International Conference on Structural Dynamics, EURODYN 2011, 2011, July, 2242-2249.

[8] Mohanan A., Pradeep K.R., Narayanan K.P., Performance assessment of sandwich structures with debonds and dents, International Journal of Scientific & Engineering Research 2013, 4, 5, 174-179.

[9] Moustapha I.M., El Mahi A., El Guerjouma R., Dazel O., Damping analysis in flexural vibration of sandwich beams with debonding, Sociélé Française d'Acaustique, 2012, April.

[10] Baba B.O., Free vibration analysis of curved sandwich beams with face/core debond using theory and experiment, Mechanics of Advanced Materials and Structures 2012, 19, 5, 350-359, DOI: 10.1080/15376494.2010.528163.

[11] Burlayenko V.N., Sadowski T., Influence of skin/core debonding on free vibration behavior of foam and honeycomb cored sandwich plates, International Journal of Non-Linear Mechanics 2010, 45, 10, 959-968, DOI: 10.1016/j.ijnonlinmec.2009.07.002.

[12] Kim H.Y., Hwang W., Effect of debonding on natural frequencies and frequency response functions of honeycomb sandwich beams, Composite Structures 2002, 55, 1, 51-62, DOI: 10.1016/S0263-8223(01)00136-2.

[13] Baba B.O., Thoppul S., Experimental evaluation of the vibration behavior of flat and curved sandwich composite beams with face/core debond, Composite Structures 2009, 91, 1, 110-119, DOI: 10.1016/j.compstruct.2009.04.037.

[14] Tsai S.N., Taylor A.C., Vibration behaviours of single/multi-debonded curved composite sandwich structures, Composite Structures 2019, 226, August, 111291, DOI: 10.1016/j.compstruct.2019.111291.

[15] Burlayenko V.N., Sadowski T., Dynamic behaviour of sandwich plates containing single/multiple debonding, Computational Materials Science 2011, 50, 4, 1263-1268, DOI: 10.1016/j.commatsci.2010.08.005.

[16] Sadeghpour E., Sadighi M., Ohadi A., Free vibration analysis of a debonded curved sandwich beam, European Journal of Mechanics, A/Solids 2016, 57, 71-84, DOI: 10.1016/j.euromechsol.2015.11.006.

[17] Tsai S.N., Taylor A.C., Vibration behaviours of single/multi-debonded composite sandwich structures with nanoparticle-modified matrices, Composite Structures 2019, 210, August, 590-598, DOI: 10.1016/j.compstruct.2018.11.071.

[18] Idriss M., El Mahi A., El Guerjouma R., Characterization of sandwich beams with debonding by linear and nonlinear vibration method, Composite Structures 2015, 120, 200--207, DOI: 10.1016/j.compstruct.2014.09.036.

[19] Tsai S.N., Vibration behaviours of multi-debonded sandwich beams with symmetric angle-ply facesheets, Journal of Composite Materials 2023, DOI: 10.1177/0021998323 1217131.

[20] Kalgutkar A.P., Banerjee S., Free vibration analysis of hygrothermally stable stiffened composite plates with plate-stiffener interfacial debonding, Mechanics of Advanced Materials and Structures 2024, January, 1-15, DOI: 10.1080/ 15376494.2024.2303726.

[21] Comsol Application Gallery, Forced Vibration Analysis of a Composite Laminate [Online], Available: https://www.comsol.com/model/forced-vibration-analysis-of-a-composite-laminate-67731.

[22] Demircioğlu U., Çakir M.T., An investigation of the influence of various shaped cutouts on the free vibration behavior of sandwich structures, Sakarya University Journal of Science 2022, August, 26, 4, 687-694, DOI: 10.16984/ saufenbilder.1063422.

[23] Kollar L.P., Springer G.S., Mechanics of Composite Structures, 1st ed. Cambridge University Press, 2003.

[24] Pushparaj P., Suresha B., Free vibration analysis of laminated composite plates using finite element method, Polymers and Polymer Composites 2016, 24, 7, 529-538, DOI: 10.1177/096739111602400712.

